Evaluation of Directional Dependence of Sensitivity for Room-Temperature Magnetic Flux Sensors With Wide Sensitivity Region

Yoshiaki Adachi (足立善昭)[1], Yuki Mizuhara (水原悠貴)[2], and Yasushi Terazono (寺園泰)[2]

[1]Applied Electronics Laboratory, Kanazawa Institute of Technology, Ishikawa 920-1331, Japan
[2]Advanced Products Development Center, TDK Corporation, Chiba 272-8558, Japan

Recently, the room-temperature (RT) magnetic flux sensors have begun to be applied to biomagnetic measurements. The RT sensors have a large advantage that they can be placed closer to the magnetic sources and obtain larger signals, unlike the superconducting quantum interference device (SQUID) flux sensors. However, when an RT sensor is placed closer to the sources, the dimension of the sensitivity region cannot be negligible, and the directional dependence of sensitivity should be considered to estimate the theoretical magnetic signals for magnetic source analysis. We proposed a method to evaluate the directional dependence of the sensitivity of the RT sensors in response to adjacent magnetic sources using the array of coils arranged along a circular arc. Consequently, it was revealed that a specific magnetoresistance device-based flux sensor with a certain spatial extent had the directional dependence of sensitivity with a bell-shaped profile. We also proposed the multiple sensitivity points model for the bell-shaped profile and estimated the sensitivity distribution over the sensitivity region, which is expected to be effective in improving the accuracy of the magnetic source analysis using an RT sensor array.

Index Terms— **Biomagnetic measurement, magnetoresistance (MR)-device-based flux sensor, room-temperature (RT) flux sensor.**

I. Introduction

BIOMAGNETIC measurement is a promising tool for the non-invasive investigation of electric activities in body tissues such as neurons or muscles. The electric currents generated by these tissues induce weak magnetic fields that can be detected using highly sensitive magnetic flux sensors arranged over the body surface. The original electric activities are estimated by conducting an appropriate magnetic source analysis of the obtained magnetic field distribution. The electric activities reflect the function of the tissues and provide significant clinical information. The two applications of the biomagnetic measurements magnetoencephalogram and magnetocardiogram that are effective for the non-invasive functional imaging of the brain and heart, respectively, are already commercialized and introduced to hospitals [1].

Recently, the performance of room-temperature (RT) magnetic flux sensors such as magnetoresistance (MR)-device-based sensors, magnetoimpedance (MI) sensors, or fluxgates has been improved and begun to be applied to detect biomagnetic fields that are extremely small and detected only using superconducting quantum interference device (SQUID) flux sensors [2]–[6]. The magnetic field resolution of the RT sensors is still inferior to the SQUID sensors. However, the RT sensors have two well-known advantages for biomagnetic measurements other than the non-necessity of cooling. One is the flexibility of the sensor arrangement, and the other is that the sensor can be placed closer to the magnetic sources because the cryostat that separates the source from the sensors is removed, unlike the SQUID sensors.

When the flux sensor and magnetic source are close to each other, a higher signal intensity can be expected because the intensity of the magnetic field increases as the distance from the source to the sensor decreases. However, if the flux sensors have a wide sensitivity region, for example, when using a flux concentrator, the directional dependence of the sensitivity must be considered. If the magnetic field $\mathbf{B}$ at the sensor position $\mathbf{r}$ is assumed to be uniform and/or the dimension of the sensor is negligibly small, the sensor sensitivity region is represented by a single point, and the theoretical output signal s from the sensor is expressed using the scalar product or $s = g|\mathbf{B}(\mathbf{r})||\mathbf{n}|\cos\theta$, where g, $\mathbf{n}$, and θ represent the sensor sensitivity, orientation of the sensor, and angle between the sensor orientation and magnetic field direction, respectively. Most algorithms used to conduct magnetic source analysis are based on this assumption. However, when the magnetic field flux sensors are placed adjacent to the sources of magnetic field and the size of the sensor is not negligible, the non-uniformity of the magnetic field to which the sensor is exposed must be considered. Consequently, the sensor sensitivity area is not represented by a single point and the theoretical output signal cannot be calculated using the scalar product. For example, in the case of a magnetic flux sensor coupled with a pickup coil to improve its sensitivity like a SQUID sensor as shown in Fig. 1(a), when the magnetic sources are positioned sufficiently far from the pickup coil, the diameter of the pickup coil (a) becomes negligible, and the theoretical magnetic signal versus θ, corresponding to the directional dependence of the sensitivity called the theta profile, traces a cosine curve. However, if the distance between the source and the pickup coil (d) is short,

Manuscript received May 6, 2020; revised June 20, 2020; accepted July 7, 2020. Date of publication July 13, 2020; date of current version January 20, 2021. Corresponding author: Y. Adachi (e-mail: adachi.y@gmail.com).

Color versions of one or more of the figures in this article are available online at https://ieeexplore.ieee.org.

Digital Object Identifier 10.1109/TMAG.2020.3008912

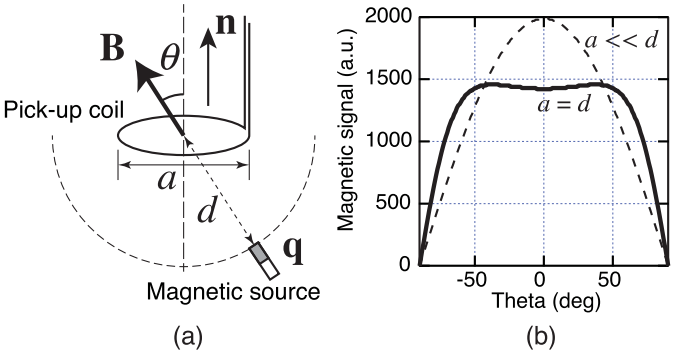

Fig. 1. (a) Model of the magnetic flux sensor coupled with a pickup coil. (b) Theta profile of the magnetic sensor coupled with a pickup coil.

the surface integral must be applied over the area of the pickup coil to obtain the theoretical magnetic signal. The theta profile does not trace the cosine curve as θ changes as shown in Fig. 1(b). For the precise estimation of the magnetic sources adjacent to the sensor, it is essential to clarify the theta profile, i.e., the directional dependence of the sensitivity.

In the case of some types of commercially available MR-based sensors, an MR element is coupled with a flux concentrator and packaged as a sensor module, whose output is linearized to the input magnetic field. The flux concentrator is made of a high-permeability metal and gathers the external magnetic field to improve the sensitivity. There are not-a-few reports showing that the directional dependence of the sensitivity of a single sensor element traces a cosine-like curve in the uniform magnetic field, for example, as indicated in [7]. However, if the dimensions of the flux concentrator coupled with the sensor element are significant compared to the distance between the sensor and magnetic source, the sensor module captures magnetic fields in a certain volume over which the magnetic fields are considered not to be uniform. The directional dependence of the sensitivity in response to the magnetic source close to the sensor module is not necessarily cosine-like. In order to obtain the theta profile in the same way as the sensor coupled with a pickup coil described in the previous paragraph, the detailed structure of the flux concentrator is necessary. However, it is not usually disclosed by the sensor manufacturer. Also, even if the design of the flux concentrator is known, obtaining the theta profile is useful for calibration purpose.

In this study, we experimentally investigated the directional dependence of the sensitivity of commercially available RT sensors. To explain the obtained theta profiles responding to an adjacent magnetic source, a model called "multiple sensitivity points model" was proposed.

II. Methods

A. Evaluation of the Theta Profile

To evaluate the theta profile of the RT sensors, a coil array was fabricated, as shown in Fig. 2. A set of 23 solenoid coils was arranged along a circular arc with the radius of 20 mm. The solenoid coil had the inner/outer diameter of 0.83/1.75 mm and the length of 30 mm. The number of turns was 1000. Each coil was oriented in the radial direction, and the angular interval between adjacent coils was 10°. A channel

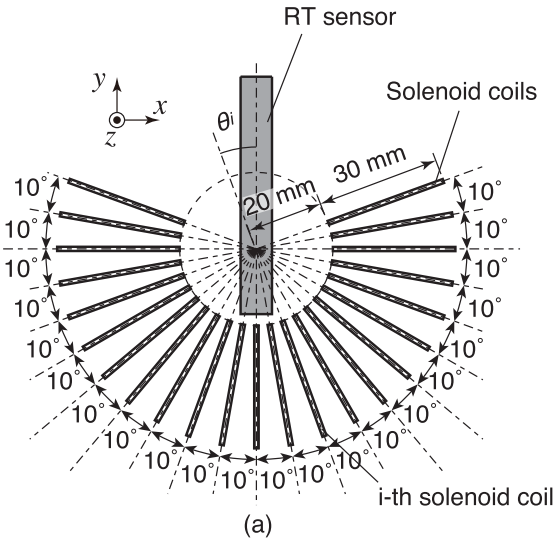

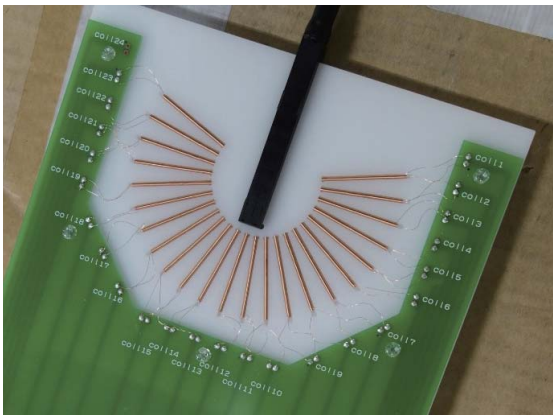

(b)

Fig. 2. (a) Schema of the coil array to evaluate the theta profile. (b) Appearance of the coil array.

was excavated along the midline ($\theta = 0°$) of the coil array. An RT sensor was inserted in the channel so that its orientation was aligned along $\theta = 0°$.

The theta profiles of two commercially available RT sensors were examined. One was an MR-based sensor (pT-MR, TDK, Japan) [8]. The outer dimension of the plastic package of the sensor module is 8 mm × 8 mm × 69 mm. The package contains an MR device coupled with a flux concentrator made of a high-permeability metal and electronics to make the sensor output linearized. However, its structure and dimension are not disclosed by its manufacturer. The other was an MI sensor (MI-CB-1DH-B, AICHI STEEL, Japan) [9]. A piece of amorphous magnetic wire core corresponds to the sensitivity region of the sensor. Its dimension is φ 0.8 mm × 6 mm.

The set of 23 coils was excited using a sinusoidal burst current with the frequency of 80 Hz for 300 ms one after another. The amplitude of the current was 0.5 mA_{pp}, and the intensity of the induced magnetic field at the sensor was estimated at several nanoteslas. The output impedance of the current driver connected to each coil was sufficiently high, and then the induced voltage in the non-excited coils adjacent to the excited one hardly affect the measurement. The sensor

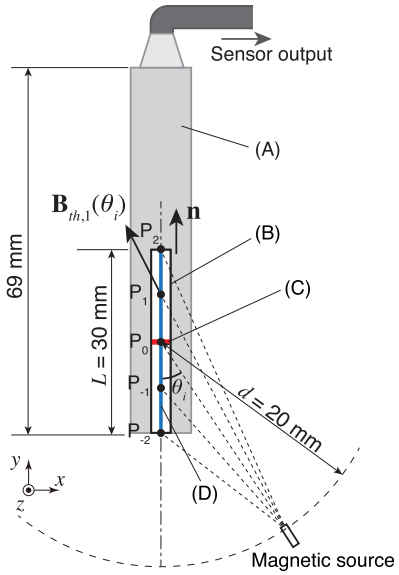

Fig. 3. Schematic of the MR-based sensor module with a flux concentrator and the multiple sensitivity points model (not in scale). (a) Sensor module package. (b) Flux concentrator. (c) Assumed sensor position, which obtained by our previous work, corresponding to the position of the MR device. (d) Assumed line segment.

was exposed to the magnetic field from different orientations with $-110° < \theta < 110°$. The position of the RT sensors was adjusted along the channel, that is, the y-axis, so that the signals from the coils at $\theta = \pm 90°$ became zero or less than the noise level. The output signal corresponding to the magnetic field from each coil was digitally recorded. The excitation sequence for 23 coils was repeated at least 64 times, and the repeatedly obtained signals were averaged to improve the signal-to-noise ratio. The 80 Hz component was extracted from the obtained signals using the fast Fourier transform. Thus, we obtained a set of 23 magnetic signals from the solenoid coils at each angle, corresponding to the theta profile $V(\theta_i)$ $(i = 0, \ldots, 22)$.

B. Multiple Sensitivity Points Model and Calibration

To understand the theta profile of the RT sensors, which did not trace the cosine curve, the multiple sensitivity points model was introduced. We assumed that the sensor was a segmented line with a certain length and assigned multiple sensing points along the line at a regular interval. Each sensing point had an individual sensitivity g_n toward the direction $\mathbf{n}$ and provided the cosine theta profile (see Fig. 3).

We estimated a set of g_n from the obtained theta profile using numerical search. The position and orientation of each solenoid coil were given in advance. When the position of the sensor was assumed, the "off-axis" theoretical magnetic field from the ith solenoid coil at the nth sensing point $\mathbf{B}_{\mathrm{th},n}(\theta_i)$ was estimated using a generalized complete elliptic integral [10], and then the theoretical signal $V_{\mathrm{th}}(\theta_i)$ was calculated as follows:

$$V_{\mathrm{th}}(\theta_i) = \sum_{n}^{N} g_n \mathbf{B}_{\mathrm{th},n}(\theta_i) \cdot \mathbf{n} \tag{1}$$

where N and $\mathbf{n}$ represent the number of the sensing points and orientation of the sensor, respectively. A set of sensitivities and the position of the sensor were obtained using the least squares method optimizing these parameters to minimize E that is determined as follows:

$$E = \sum_{i} |V_{\mathrm{meas}}(\theta_i) - V_{\mathrm{th}}(\theta_i)|^2 \tag{2}$$

where $V_{\mathrm{meas}}(\theta_i)$ is the obtained magnetic signal from the ith coil described in Section II-A.

Preliminarily, we applied the numerical search described above, setting the number of the sensing points to 3, 5, 7, 9, and 11. When we assumed the number of the sensing point to be 5, we obtained the most stable result from the numerical search. Therefore, the number of sensing points was determined to be 5 in this study.

Here, by applying the variable separation, we introduced the base sensitivity g and the relative sensitivity u_n represented by $g_n = g u_n$, providing $\sum u_n = 1$, and calculated

$$B_{\mathrm{th},i} = \sum_{n=-2}^{2} u_n \mathbf{B}_{\mathrm{th},n}(\theta_i) \cdot \mathbf{n} \tag{3}$$

to find a set of u_n and the position of the sensor to minimize

$$E' = 1 - \frac{(\mathbf{B}_{\mathrm{th}} \cdot \mathbf{V}_{\mathrm{meas}})^2}{|\mathbf{B}_{\mathrm{th}}|^2 |\mathbf{V}_{\mathrm{meas}}|^2} \tag{4}$$

instead of E. $\mathbf{B}_{\mathrm{th}}$ and $\mathbf{V}_{\mathrm{meas}}$ are the vectors, where $\mathbf{B}_{\mathrm{th}} = [B_{\mathrm{th},0}, B_{\mathrm{th},1}, \ldots, B_{\mathrm{th},22}]$ and $\mathbf{V}_{\mathrm{meas}} = [V_{\mathrm{meas}}(\theta_0), V_{\mathrm{meas}}(\theta_1), \ldots, V_{\mathrm{meas}}(\theta_{22})]$.

We did not know the detailed structure of the flux concentrator, but we assumed the length of the line segment L to be 30 mm as shown in Fig. 3 for the following reason. When we calibrated the sensor array composed of the same MR-based sensors using a set of calibration coils arranged relatively away from the sensor array [11], assuming the sensing area as a single point, the sensing point of each sensor was localized approximately 15 mm away from the one end of the sensor module package. Assuming that the flux concentrator had a symmetric structure, the sensing point should be localized at the center of the flux concentrator. Therefore, L was set to 30 mm.

We examined the theta profiles of six MR-based sensors and estimated their sensitivity based on the multiple sensitivity points model to check their variability.

III. Results and Discussion

Fig. 4 shows the obtained theta profiles of the MR-based sensor and MI sensor. As shown in Fig. 4(a), the theta profile of the MR-based sensor does not trace a cosine curve but a bell-shaped curve. This theta profile indicates that the flux concentrator effectively collected the magnetic field oriented in the assumed sensor direction ($\theta = 0°$) more than the magnetic field on the side of the sensor. When we estimated the theoretical magnetic field from the source adjacent to the MR-based sensor, the directional dependence of the sensitivity should be considered. Meanwhile, the theta profile of the MI sensor shows the cosine-like shape, as shown in Fig. 4(b), because the sensitivity region of the MI sensor is sufficiently small compared to the distance between the magnetic source and the sensor.

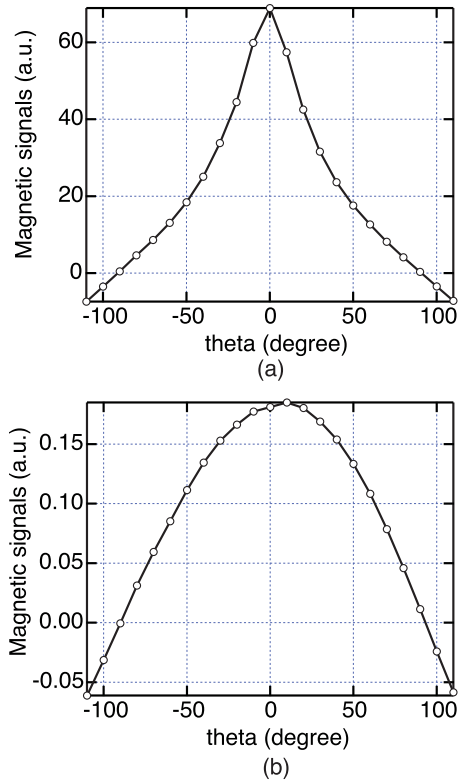

Fig. 4. Obtained theta profiles of (a) MR-based sensor and (b) MI sensor.

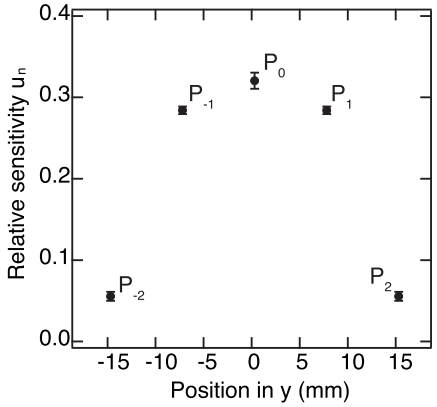

Fig. 5. Distribution of relative sensitivity of MR sensors. Labels in the plot correspond to the positions indicated in Fig. 4. Error bars represent the standard deviation.

After obtaining the theta profiles of six MR sensors, the sets of the relative sensitivities u_n and sensor position to minimize E' in (4) were estimated assuming the multiple sensitivity points model under the constraints $u_2 = u_{-2}$ and $u_1 = u_{-1}$, while considering the symmetrical structure of their flux concentrator. Fig. 5 shows the plot of the averaged relative sensitivity and its variability along the sensitivity region of the MR sensor. According to the estimated distribution, the sensitivity at the center of the sensitivity region is relatively higher than at both ends.

Using the set of the relative sensitivity shown in Fig. 5 and (1), the theoretical theta profiles were estimated when the distance between the center of the sensitivity region and magnetic source was assumed to be 20, 40, 80, and 160 mm. Fig. 6 shows the estimated theoretical theta profiles for the

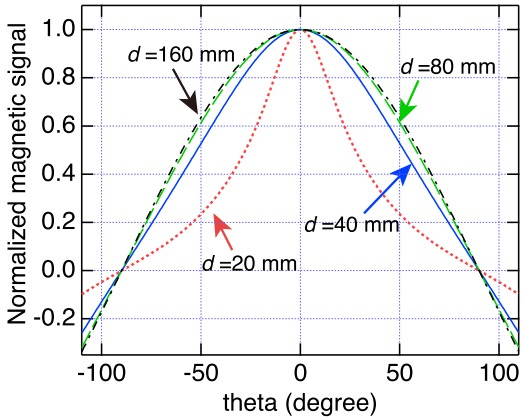

Fig. 6. Estimated theoretical theta profile. Each plot was normalized by the value at $\theta = 0°$. Red dotted, blue solid, green dashed, and black dashed-dotted lines represent the theta profiles for the magnetic sources at 20, 40, 80, and 160 mm, respectively.

magnetic sources at various distances. The plot for $d = 20$ mm shows the bell-shaped profile corresponding to Fig. 4(a). In contrast, when $d = 40$ mm or above, the theta profiles show cosine-like curves approximately. This indicates that if we apply the scalar product to the analysis of the magnetic sources placed at more than 40 mm from the sensor, for example, in the case of magnetocardiogram, the effect of the wide sensitivity region would not be significant. The magnetic fields over the sensitivity region could be regarded as approximately uniform.

However, when the source of the magnetic field is positioned at a distance of less than 20 mm, as is the case when targeting peripheral nerves or skeletal muscles, we will need to consider the bell-shaped theta profile of the MR-based sensor and application of the multiple sensitivity points model to magnetic source analysis because the depth of these magnetic sources is often less than 10 mm from the body surface.

In biomagnetic measurements, a set of small coils attached to the anatomical points of the body surface of subjects, called marker coils, is often used to determine the position of the subject relative to the sensor array [12]. The marker coils induce specific magnetic fields that can be detected using a sensor array, and the position of the marker coils relative to the sensor array is estimated from the detected magnetic field distribution using a source localization algorithm. Herewith, the position of the subject relative to the sensor array is obtained via the position of the marker coils. These coils are usually in close contact with the sensor array because they are attached to the body surface of the subjects. The distance between the marker coils and sensors should be less than 20 mm. Therefore, while applying the marker coil localization to the biomagnetic measurement using the array of the MR-based sensors, the bell-shaped theta profile should be considered. Otherwise, the marker coil localization and source reconstruction based on the result of the marker coil localization will include an indispensable error.

The method to evaluate the directional dependence of the sensitivity and the multiple sensitivity points model proposed in this study will also be effective for other magnetic flux sensors with wide sensitivity regions such as an orthogonal fluxgate [13].

The similar approach to the multiple sensitivity points model proposed in this study is also effective for SQUID magnetometers with a pickup coil. As mentioned in Section I, when the magnetic source locates adjacent to the sensor, we need to apply the surface integral over the area of the pickup coil to estimate the theoretical magnetic fields. However, the computational cost of the surface integral is quite high and often makes the magnetic source analysis time consuming. We can reduce the computational cost by applying the multiple sensitivity points model instead of the surface integral when a number of sensitivity points are arranged in the area of the pickup coil.

IV. Conclusion

In this article, we proposed a method to evaluate the directional dependence of the sensitivity of an RT magnetic flux sensor when the magnetic sources are located quite adjacent to the sensor. The specification of the directional dependence of commercially available sensors provided by their manufacturers is often evaluated in a uniform magnetic field and not suited for the biomagnetic applications because the distance between the sensor and the source is quite short and the magnetic field over the sensor sensitivity region cannot be regarded as uniform. Using the proposed method, it clearly revealed that the directional dependence of the sensitivity of the tested MR-based sensors had the bell-shaped profile that was different from the MI sensor, even if the structure of the flux concentrator in the sensor module package was unknown. The multiple sensitivity points model for the RT sensors and estimation of a set of the relative sensitivities would be effective in analyzing the directional dependence of the sensitivity even though the assumption for the structure of the flux concentrator was less rigorous. This model is expected to improve the accuracy of the analysis of the magnetic sources adjacent to the sensors, for example, marker coil localization for biomagnetic measurements with the RT sensor array. The accuracy improvement of the magnetic source analysis based on the multiple sensitivity points model and the validity of the model itself will be evaluated as our future issues.

Acknowledgment

This work was supported in part by KAKENHI, Japan Society for the Promotion of Science, under Grant 18K12044.

The authors would like to thank TDK Corporation, Ichikawa, Japan, for lending their MR-device-based flux sensors. They would also like to thank Editage for the English language editing service.

References

[1] R. L. Fagaly, "Superconducting quantum interference device instruments and applications," *Rev. Scientific Instrum.*, vol. 77, no. 10, Oct. 2006, Art. no. 101101.

[2] Y. Shirai *et al.*, "Magnetocardiography using a magnetoresistive sensor array," *Int. Heart J.*, vol. 60, no. 1, pp. 50–54, Jan. 2019, doi: 10.1536/ihj.18-002.

[3] M. Wang, Y. Wang, L. Peng, and C. Ye, "Measurement of triaxial magnetocardiography using high sensitivity tunnel magnetoresistance sensor," *IEEE Sensors J.*, vol. 19, no. 21, pp. 9610–9615, Nov. 2019, doi: 10.1109/JSEN.2019.2927086.

[4] T. Uchiyama, S. Nakayama, K. Mohri, and K. Bushida, "Biomagnetic field detection using very high sensitivity magnetoimpedance sensors for medical applications," *Phys. Status Solidi (A)*, vol. 206, no. 4, pp. 639–643, Apr. 2009, doi: 10.1002/pssa.200881251.

[5] Y. Ogata, T. Tanaka, Y. Hata, B. Kakinuma, T. Ueda, and K. Kobayashi, "Study of spatial filter for magnetocardiography measurements without a magnetically shielded room," *Adv. Biomed. Eng.*, vol. 8, pp. 170–176, 2019, doi: 10.14326/abe.8.170.

[6] H. Karo and I. Sasada, "Magnetocardiogram measured by fundamental mode orthogonal fluxgate array," *J. Appl. Phys.*, vol. 117, no. 17, May 2015, Art. no. 17B322.

[7] Y. Nishibe, H. Yamadera, N. Ohta, K. Tsukada, and Y. Nonomura, "Thin film magnetic field sensor utilizing magneto impedance effect," *Sens. Actuators A, Phys.*, vol. 82, nos. 1–3, pp. 155–160, May 2000.

[8] *Capable of Detecting Extremely Weak Biomagnetic Signals at Room Temperature*. Accessed: Aug. 27, 2018. [Online]. Available: https://product.tdk.com/info/en/techlibrary/developing/bio-sensor/index.html

[9] *MI Sensor, Highly Sensitivity/Small Size/Low Power Consumption Magnetic Sensor*. Accessed: Apr. 25, 2020. [Online]. Available: https://www.aichi-mi.com/e-home-new/highly-sensitive-magnetometers/type-dh/

[10] N. Derby and S. Olbert, "Cylindrical magnets and ideal solenoids," *Amer. J. Phys.*, vol. 78, no. 3, pp. 229–235, Mar. 2010, doi: 10.1119/1.3256157.

[11] Y. Adachi, D. Oyama, Y. Terazono, T. Hayashi, T. Shibuya, and S. Kawabata, "Calibration of room temperature magnetic sensor array for biomagnetic measurement," *IEEE Trans. Magn.*, vol. 55, no. 7, pp. 1–6, Jul. 2019.

[12] S. N. Erné, L. Narici, V. Pizzella, and G. L. Romani, "The positioning problem in biomagnetic measurements: A solution for arrays of superconducting sensors," *IEEE Trans. Magn.*, vol.-23, no. 2, pp. 1319–1322, Mar. 1987.

[13] I. Sasada, "Orthogonal fluxgate mechanism operated with DC biased excitation," *J. Appl. Phys.*, vol. 91, no. 10, pp. 7789–7791, 2002, doi: 10.1063/1.1451899.